

A Novel Alignment Procedure and Results for the LHCb Silicon Tracker Detector

Frédéric Dupertuis

Laboratoire de Physique des Hautes Energies, Ecole Polytechnique Fédérale de Lausanne, Switzerland
on behalf of the LHCb Silicon Tracker and Alignment groups

Abstract—The LHCb experiment is designed to perform high-precision measurements of CP -violation and rare decays of B hadrons at the Large Hadron Collider. The Silicon Tracker (ST) is a silicon strip detector intended to precisely measure the particle trajectories produced by proton-proton interactions. It has a total sensitive area of about 12 m^2 around the beam axis. The Silicon Tracker has a single hit resolution better than $60 \mu\text{m}$ that put strict constraints on its alignment. The current alignment procedure is demonstrated to be fast, robust and able to achieve a suitable alignment precision. Two novelties have been added to the method to improve significantly the alignment accuracy using tracks from vertex- and mass-constrained resonances and as well as track extrapolation with magnet off data. Selected results demonstrating alignment improvements are presented.

I. INTRODUCTION

LHCb is an experiment dedicated to b and c physics studies at the LHC. The aim is to perform precision measurements of CP -violation and rare decays in b and c hadron systems. The $b\bar{b}$ quark pairs at LHC are incoherently produced at low polar angle in the forward and backward direction (Fig. 1) and this motivates the LHCb forward geometry. LHCb reconstruction performance is sensitive to pile-up. The optimal instantaneous luminosity for LHCb is below the maximum luminosity the LHC can achieve ($\mathcal{L}_{LHC} = 10^{34} \text{ cm}^{-2} \text{ s}^{-1}$) and can be tuned with beam optics. In 2011 LHCb has been operating at an instantaneous luminosity of $3.5 \cdot 10^{32} \text{ cm}^{-2} \text{ s}^{-1}$.

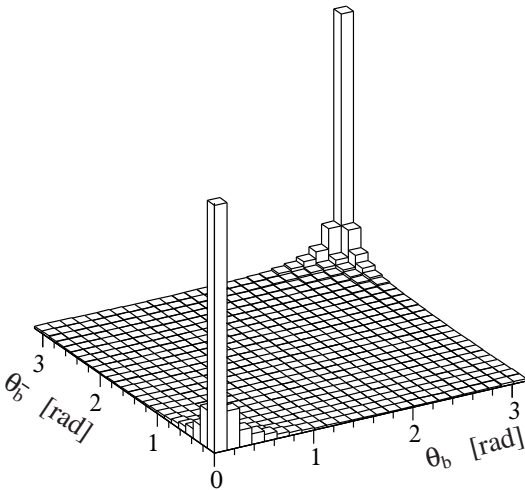


Fig. 1. $b\bar{b}$ quark pair production at LHC.

II. THE LHCb EXPERIMENT

The LHCb experiment [1] is a single-arm spectrometer located along the LHC collider ring. The vertexing and tracking detector around the interaction point is called the Vertex LOcator (VELO) and is made of n -on- n R and ϕ silicon micro-strip sensors. In order to get a high precision vertex reconstruction VELO sensors are positioned at a minimal sensitive distance to the beam of 8.2 mm. To protect the sensors from beam movements during injection, the sensors are placed in two detector halves that can be individually moved away from the beam line. The reproducibility of the position of the detectors between subsequent closings is better than 10 micron.

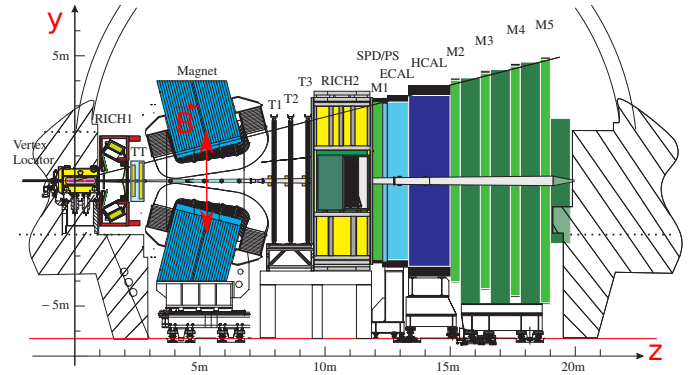


Fig. 2. View of the LHCb detector in the y - z plane.

Charged particle momentum is measured by bending the tracks with a 4 Tm warm dipole magnet with a maximum intensity of 1.1 T. In addition to the VELO, the tracking system is composed of the Tracker Turicensis (TT) and three T stations (T1, T2, T3) located upstream and downstream the magnet respectively. The T stations are made of two sub-detectors, the Inner Tracker (IT) which covers the inner region and the Outer Tracker (OT) that surrounds the IT. The TT and IT form the Silicon Tracker (ST), and are both composed of silicon micro-strip to handle high track multiplicity around the beam pipe. More details about TT and IT will be given in the next section. To achieve a good spatial resolution at a reasonable cost and cover a required area of 340 m^2 , the OT is based on gaseous straw-tubes detectors.

Two Ring Imaging Cherenkov detectors (RICH) are used for particle identification. The first one is located between the VELO and TT and makes use of Aerogel- C_4F_{10} and the second one just after the T stations uses CF_4 as radiator. A

good K/π separation for a particle momentum range of 1 to 150 GeV is obtained.

The calorimeter system consists of a Scintillating Pad Detector (SPD), a PreShower detector (PS), an Electromagnetic CALorimeter (ECAL) and Hadronic CALorimeter (HCAL). The SPD allows to discriminate between charged and neutral particles. The PS detects the showers developed in a lead converter using scintillators, allowing e^\pm/π^\pm discrimination. The ECAL is made of lead and scintillator, and is optimised to reconstruct π^0 and γ from B decays. The HCAL, a sandwich of steel and scintillator, provides hadron identification. The full calorimeter system is located after the second RICH detector.

Finally five muon chambers, M1 to M5, are used to track muons and provide muon identification. They are the last subdetectors downstream the magnet except for M1 which is located inbetween RICH2 and the calorimeter system. Multiwire proportional chambers are used apart from the inner part of M1 which uses triple GEM detectors.

III. THE SILICON TRACKER

The IT and TT are both made of p-on-n HPK silicon micro-strip sensors from Hamamatsu. Since they are exposed to high track multiplicity, both subdetectors are kept cool at an operating temperature of 0°C to minimise radiation damage and avoid thermal runaway.

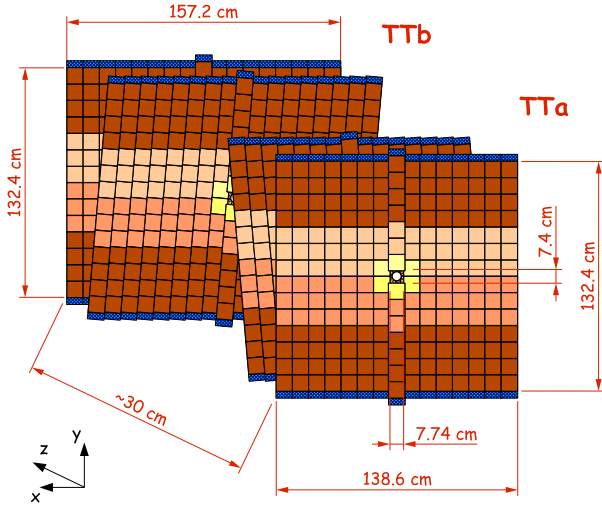


Fig. 3. The TT layout with its four layers where each rectangle unit is a silicon sensor and in dark blue is the front-end electronics.

The four layers in the TT and in each of the three IT stations are arranged in an X-U-V-X configuration, where the X layers are vertical (0° relative to the vertical axis), and the U and V "stereo" layers are rotated by $+5^\circ$ and -5° , respectively. The TT covers an area of about 7.9 m^2 .

The TT readout modules contain from one to four bonded silicon sensors (Fig. 4). This results in readout strips up to 37 cm long. The micro-strips pitch is $183\ \mu\text{m}$ and the sensors thickness is $500\ \mu\text{m}$. In total, this gives 143360 readout channels.

The IT is separated in three stations where each station is composed of four boxes and each box has four layers made

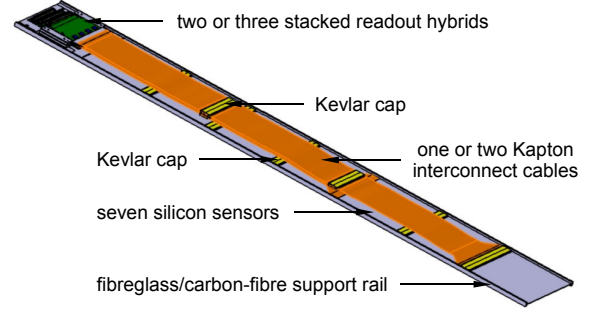


Fig. 4. A TT half-module layout with 4-2-1 silicon sensors readout modules.

of seven readout modules (Fig. 5). The IT covers an area of about 4.2 m^2 . The boxes above and below the beampipe are made of single-sensor modules whereas side boxes are made of two bonded silicon sensors.

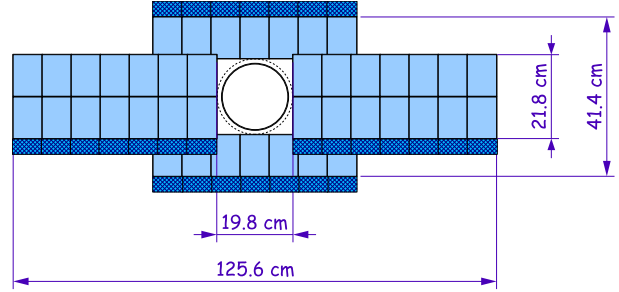


Fig. 5. The first IT station layout where only one layer is shown. In light blue are the sensors, and in dark blue is the front-end electronics.

The IT micro-strip pitch is $198\ \mu\text{m}$ and the sensor thickness is 320 (410) μm for single (double) silicon sensor(s) modules (Fig. 6). In total, the IT has 129024 readout channels.

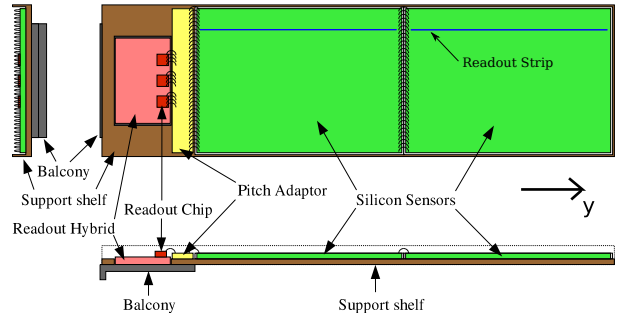


Fig. 6. A two bonded silicon sensors (long) IT module layout.

IV. DETECTOR ALIGNMENT PROCEDURE

A. Silicon Tracker Survey

During the assembly and after installation of the TT and IT in the LHCb cavern, survey measurements were performed. These measurements were the initial position of the sensors and they were stored into the LHCb geometry database.

To profit from the excellent resolution of the detector, the tracker must be aligned well below its single hit resolution which is better than $60\ \mu\text{m}$ for the ST. For the TT system and

IT boxes position, the survey accuracy is about 1 mm, which is clearly not sufficient for our physics needs.

B. LHCb Software Alignment

The required accuracy can be achieved using track-based alignment. The LHCb alignment procedure is based on a global chi-square (χ^2) minimization of both alignment and track parameters [2]-[4] specially adapted to the standard LHCb track model, making use of a Kalman filter [5]. The procedure and its implementation into the LHCb Gaudi framework have been presented during the 2008 IEEE Nuclear Science Symposium using misaligned MC and very first cosmic data [6]. Key points of the procedure are given below.

For each track, a χ^2 is evaluated from track fit residuals as:

$$\chi^2 = [m - h(x)]^T V^{-1} [m - h(x)] \quad (1)$$

where m is the measurement vector, h the measurement model vector, V the correlation matrix and x the track parameters. $r(x) = m - h(x)$ is called the residual.

An extension of the measurement model with a set of alignment parameters α can be considered: $h(x) \rightarrow h(x, \alpha)$. The total χ^2 minimisation of a track sample with respect to both track and alignment parameters can be expressed as:

$$0 \equiv \frac{d\chi^2}{d\alpha} \quad (2)$$

To account for non-linear measurement model vector h , an iterative solution using the Newton-Raphson method is used. Changes in alignment parameters α from a set of initial alignment values α_0 are given by:

$$\Delta\alpha \equiv \alpha - \alpha_0 = - \left(\frac{d^2\chi^2}{d\alpha^2} \right)^{-1} \bigg|_{\alpha_0} \frac{d\chi^2}{d\alpha} \bigg|_{\alpha_0} \quad (3)$$

Effort has been put to use in the alignment the same track model as in the reconstruction fitter [5].

Until 2010, the LHCb software alignment was performed using a set of high momentum tracks satisfying some quality requirements such as track fit χ^2 and number of hits on the track. We describe next an improved selection of tracks and new constraints that can be used by the alignment.

C. Tracks from Vertex and Mass-constrained Resonances

It was observed that the use of unconstrained high-momentum tracks in the alignment result in poorly constrained global degrees of freedom (DOF) of the geometry. This is for example illustrated in the x-translation (T_x) of the two halves of the VELO because of insufficient constraints connecting the two parts of the detector. More generally, when the residuals are only weakly sensitive to degrees of freedom, the corresponding alignment parameters are called weak modes. In the case of the VELO, the T_x alignment can be performed efficiently when pairs of tracks are constrained to originate from a common vertex. This allow to connect otherwise independent parts of the detector. T_x and other DOFs can also be constrained by using the residuals from sensor modules overlapping on the particle trajectories. However, larger data

samples are needed to take advantage of this feature, since only a small fraction of tracks have hits on overlapping sensors.

A second weak point is the non-negligible probability to have wrong hits added to the track leading to so-called ghost tracks. The alignment procedure is sensitive to the effect of these non-physical tracks that clearly decrease the alignment quality. We suppress ghost tracks by using daughter tracks from a cleanly selected sample of $J/\psi \rightarrow \mu^+\mu^-$ or $D^0 \rightarrow K^-\pi^+$. The ghost track rate decreased significantly with the J/ψ and becomes almost negligible with the D^0 . But some issues remain such as the T_x alignment of the T stations which is identify as a weak mode. The idea to constrain the daughter tracks invariant mass to the known resonance mass has been found. Practically, this procedure helps to constrain the curvature of the tracks and get ride of the T_x weak mode. Additional benefits of these constraints are the addition of correlations between distant detector elements which allows the constraint of additional global DOFs. The alignment algorithm convergence has also been found to be faster and less tracks are needed than in the previous alignment procedure.

Vertex and mass constraints are added to the alignment procedure based on a Kalman filter as described in [5].

D. Alignment Results

The mass resolution is significantly improved by the new alignment technique. Figure 7 presents the J/ψ mass spectrum using an alignment performed with tracks from vertex- and mass-constrained $D^0 \rightarrow K^-\pi^+$ and with high momentum tracks. Two Crystal Ball (CB) functions with the same mean, α , n_0 are fitted to each distribution. The width of the dominant CB shows a clear improvement from 16.0 ± 0.2 MeV/c² to 10.5 ± 0.1 MeV/c² in the J/ψ mass resolution.

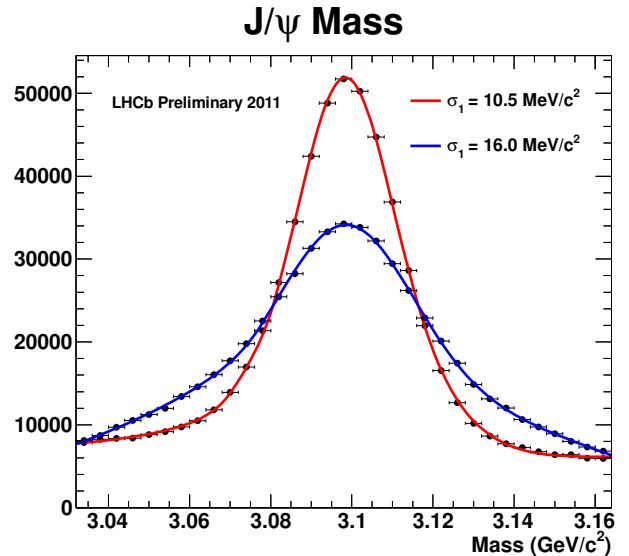


Fig. 7. J/ψ mass with an alignment performed using random high momentum tracks in blue and tracks from vertex- and mass-constrained D^0 resonance in red.

V. TRACK EXTRAPOLATION WITH MAGNET OFF DATA

A. Y Alignment with LHCb Software Alignment

The vertical position (Y) of tracks in LHCb is obtained using a combination of X and Stereo measurements. This introduces what we identify as a weak mode in the alignment: relative T_x shift of an X-type module with respect to a Stereo module is almost indistinguishable from a T_y shift of both modules. To partially solve the ambiguity, the survey constraints are used, but the competition between relative X ($\sigma_{\Delta X} \sim 100 \mu\text{m}$) and absolute Y ($\sigma_Y \sim 1 \text{mm}$) survey position accuracies can lead to unphysical vertical movements of up to 4 mm.

B. ST relevant insensitive regions perpendicular to Y axis

In order to motivate the new Y alignment procedure a deeper look into the ST geometry is needed. Each silicon sensor is surrounded by guard rings that lead to an inactive peripheral width of 1.37 mm for TT and 1 mm for IT. In addition, readout modules with more than one silicon sensor, have a bond gap of 0.15 mm between sensors.

We use these features to identify insensitive regions (edges and gaps) in the measured Y-hit spectrum.

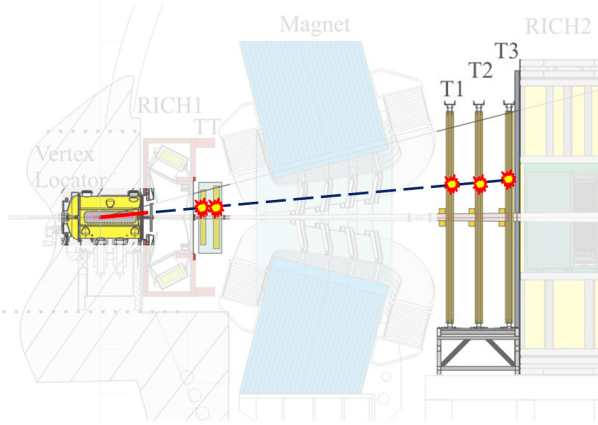


Fig. 8. VELO segment extrapolation using data without magnetic field.

C. Y Alignment using Track extrapolation with Magnet Off data

The new Y-alignment procedure uses measurements of the sensors' inefficient regions (edges and gaps) location to determine the exact position of the sensors. This can be done at LHCb with VELO track segments extrapolated to the Silicon sensors using data recorded without magnetic field (Fig. 8).

Since the TT is close from the VELO, track extrapolation resolution is good enough to see and fit the intermodule gaps. On the other hand, the IT is 8 to 10 m downstream the VELO and in this case not all IT modules present sharp gaps in the Y hits distribution. The strategy to fit gaps for more than one silicon sensor TT module and edges for single sensor TT and IT modules has been chosen. In both cases error functions are chosen to fit the hit distributions (Fig. 9) from which we can obtain the Y alignment measurement.

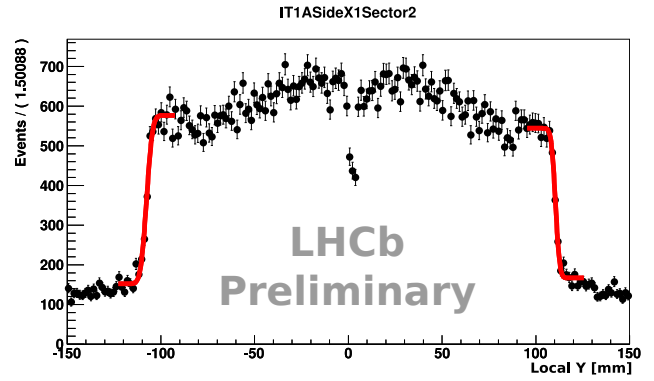


Fig. 9. Y hit distribution of a long IT module where error functions are used to fit the edges.

D. IT Active Length

One important output and cross-check of the method is the IT active length. It is the distance between the two error functions that describe the sensor edges. An active length of 108 mm and 218.15 mm is expected for respectively one and two IT silicon sensor modules. Figure 10 shows the IT active length results, which are on average within 100-150 μm of expectations:

[mm]	Short Module	Long Module
Expectation	108	218.15
Measurement	108.10 ± 0.02	218.32 ± 0.02

The discrepancy between measurements and expectations may come from a bias in the function used to describe the edges, Z misalignments of the IT boxes or/and a Z misalignment of the VELO. Investigation is going with a large sample of simulated events.

E. Y Alignment Results

Figure 11 shows TT/IT readout modules Y position relative to survey. Merging results by IT boxes and overall TT, Y misalignments are found to be no larger than 1 mm with a statistical error smaller than 100 μm , using the 20 million events recorded by LHCb without magnetic field. Moreover the quoted Survey accuracy for IT boxes and TT system is also $\pm 1 \text{mm}$, therefore Y measured misalignments are within expectations. With simulated events, it has been found that the method has a systematic error smaller than 200 μm for the IT boxes and TT system measurements.

VI. LHCb ALIGNMENT STRATEGY

First the VELO is internally aligned with VELO segments in addition to tracks crossing the two halves overlaps and with vertex constraint. In 2011, an excellent VELO internal alignment using beam gas events and satellite collisions has been achieved. Secondly, the Y alignment of the tracker (IT, TT, OT) using data without magnetic field is performed at that stage since vertical alignment method completely depends on VELO alignment. Thirdly, the global alignment is performed for the tracker with tracks from vertex- and mass-constrained resonances. Finally the RICH mirrors are aligned.

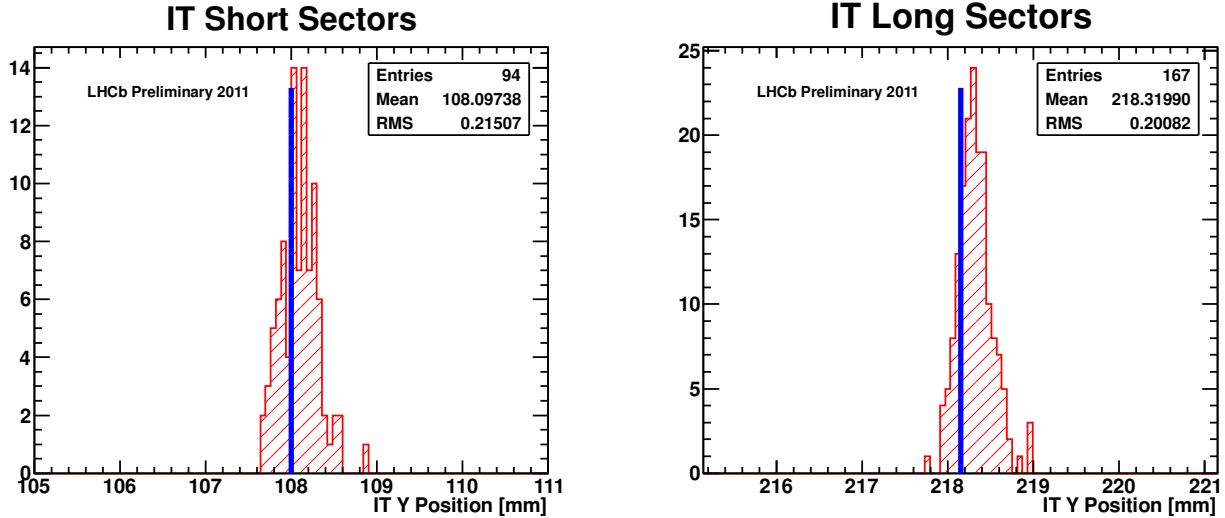


Fig. 10. Measured active length for the IT short (left) and long (right) modules. The blue vertical lines shows the expected value.

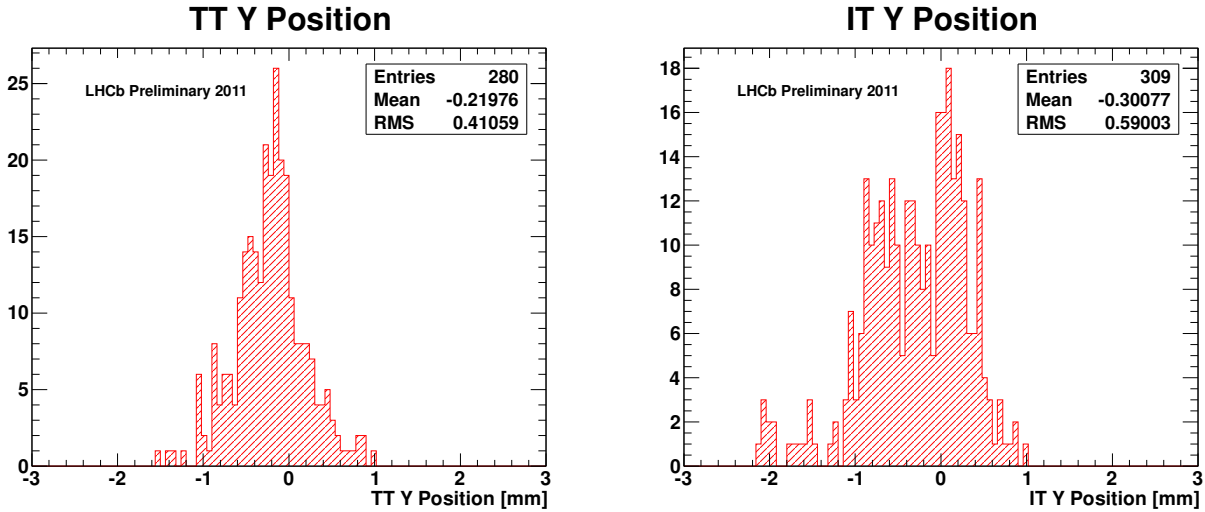


Fig. 11. Y misalignment results for the TT (left) and IT (right) modules.

VII. CONCLUSION

A novel alignment has been presented using tracks from vertex- and mass-constrained resonances for the global alignment of the LHCb tracker. In addition, the vertical alignment of the tracker has been improved using VELO tracks extrapolated with magnet-off data. A clear improvement in the J/ψ mass spectrum has been obtained. The Y-alignment method could reproduce the expected IT active length within 100-150 μm , and confirm the 1 mm vertical survey accuracy. Finally the IT boxes and overall TT are aligned within 200 μm .

REFERENCES

- [1] The LHCb Detector at the LHC. *Journal of Instrumentation*, 2008 JINST 3 S08005.
- [2] V. Blobel, *Software alignment for tracking detectors*, NIM A **566** (2006) 5.
- [3] P. Bruckman, A. Hicheur and S. J. Haywood, *Global χ^2 approach to the alignment of the ATLAS silicon tracking detectors*, ATLAS-INDET-PUB-2005-002 (2005).
- [4] A. Bocci and W. Hulsbergen, *TRT alignment for SRI cosmics and beyond*, ATL-COM-INDET-2007-011 (2007).
- [5] W. Hulsbergen, *The global covariance matrix of tracks fitted with a Kalman filter and an application in detector alignment*, NIM A **600** (2009) 471.
- [6] Louis Nicolas, Adlène Hicheur, Matthew Needham, Jan Amoraal, Wouter Hulsbergen and Gerhard Raven, *Alignment of LHCb tracking stations with tracks fitted with a Kalman filter*, CERN-LHCb-2008-066 (2008).